DESIGN AND EXPERIMENT OF HIGH-PRECISION AUTONOMOUS POSITIONING SYSTEM FOR THE MULTI-CROP COMBINED HARVESTER

/

多作物联合收获机高精度自动定位系统的设计与试验

Xiaolian LÜ[1)], Yang ZHANG[2)], Xiaohu CHEN[2)], Xiaorong LÜ[*2)]

[1)] College of Mechanical and Electrical Engineering, Chuzhou University, Chuzhou, Anhui, 239000, China;

[2)] College of Machinery & Electronics, Sichuan Agricultural University, Yaan, Sichuan, 625014, China

** Corresponding author, E-mail: lxrxj2008@163.com*

DOI: https://doi.org/10.35633/inmateh-78-44

Keywords: *Multi-Crop Harvester, NRTK, Coordinate Conversion, Multi-Sensor Information Fusion, System Testing*

ABSTRACT

Aiming at the problems of poor adaptability and low operational safety of agricultural machinery in hilly and mountainous areas, this study conducts the design and experimental research on a high-precision autonomous positioning system for the multi-crop combined harvester. The Beidou and Inertial Measurement Unit (IMU) high-precision positioning system based on Network Real-Time Kinematic (NRTK) was designed, and the hardware selection and software development of the autonomous positioning system were completed. The NRTK fixed base station in complex field environments was deployed Based on 4G communication, and dynamic differential calculations were performed with the random positions of the machinery to accurately obtain positioning data. Using the STM32L475 chip as the core information processor, efficient processing of real-time position information of combined harvester was realized based on coordinate conversion and attitude error correction of the autonomous positioning system. Performance tests were carried out using a self-developed the combined harvester. The results show that: the positioning error of the designed autonomous positioning system is less than 2 cm; when the harvester's speed ranges from 0.4 to 1.2 m/s, the maximum speed measurement error is less than 0.05 m/s, and the average speed measurement error is approximately 0.014 m/s, which meets the autonomous positioning accuracy requirements of the machinery.

摘要

针对丘陵山区农机具适应性差、作业安全性低等问题，进行了多作物联合收获机高精度自动定位系统的设计与试验研究。设计了基于网络 RTK 的北斗+IMU 高精度定位系统，完成了定位系统的硬件选型及软件开发。基于 4G 通信，通过 Web 网页部署复杂田间环境下网络 RTK 固定基站，在与机具随机位置进行动态差分运算，精确获取定位数据；以 STM32L475 芯片作为信息核心处理器，在收获机定位系统的坐标转换以及姿态误差修正的基础上，实现收获机作业中实时位置信息的高效处理。以自主研发的联合收获机为载体进行性能测试，结果表明：设计的导航系统的定位误差小于 2cm，在收获机车速 0.4~1.2m/s 范围内，最大测速误差小于 0.05m/s，平均测速误差约为 0.014m/s，满足机具田间作业时的精度需求。

INTRODUCTION

With the diversified development of agricultural planting structures, multi-crop intercropping, rotation, and other cropping patterns have been extensively promoted, which puts forward higher requirements for the versatility and operation accuracy of agricultural equipment. Under multi-crop planting patterns, the complex crop layout, variable row spacing, and differences in field terrain necessitate frequent adjustments during harvester operations, thus imposing extremely high demands on the operating skills of drivers. Manual driving is susceptible to factors such as fatigue and experience, making it difficult to guarantee operation accuracy. Meanwhile, due to the shortage of rural labor force and high labor costs, there is an urgent need for agricultural machinery with higher intelligence and more precise operation in agricultural production *(Chen et al., 2024; Choi et al., 2024; Meng et al., 2023)*. The emergence of agricultural machinery autonomous driving technology has effectively addressed the dependence of crop harvesting on manual operations, enabling precise control of operation paths and adaptation to field working environments of different crops.

Xiaolian LÜ, Prof.; Yang ZHANG, M.S. Stud; Xiaohu CHEN, M.S. Stud; Xiaorong LÜ, Prof.

Precision positioning serves as the core technology for realizing autonomous driving, therefore constructing a high-precision positioning system has become the key to improving the quality and intelligence level of harvesting operations *(Hammou et al., 2025; Saha et al., 2022; Schütte et al., 2023)*. Currently, the mainstream positioning technology is centered on Beidou/GPS multi-satellite fusion positioning, combined with augmentation technologies such as RTK, and further integrated with wireless communication technologies including inertial navigation and vision to form a multi-source fusion positioning system. Although some of these technologies have been applied to a certain extent in large-scale and standardized farmland operations, their adaptability and reliability in complex farmland environments still need to be improved *(Raikwar et al., 2022; Zhang et al., 2025; Chen et al., 2025; Udompant et al., 2021)*. *Zhao et al (2024)* from the Hubei Institute of Surveying and Mapping Engineering presents a review and analysis based on BDS+5G navigation and location service technology, and discusses its technical principles, key technologies. *Yang et al (2024)* from the Nanjing Agricultural University fused visual, GNSS, and INS data, obtaining high-precision positioning results with a mean position error of 1.77 cm and a heading error of 0.99°. *Xiao et al (2022)* from South China Agricultural University adopted Ultra-wideband (UWB) technology for real-time positioning of operating machinery, calculated the three-dimensional precise position coordinates of positioning tags through a position solution algorithm, and corrected positioning errors using a position correction algorithm. *Zhong et al (2021)* from Tongji University designed an integrated navigation system for intelligent agricultural machinery based on the Global Navigation Satellite System (GNSS) and Inertial Navigation System (INS), which realizes real-time correction of INS errors via Kalman filtering and calculates the precise position, velocity, and attitude information of agricultural machinery. *He et al (2022)* from Luo Xiwen's team conducted research on rice seedling row recognition by fusing vision and Lidar technologies, designed a rice transplanter autonomous driving tracking control system with a lateral deviation standard deviation of 4.3 cm and a heading deviation standard deviation of 3.38°. *Qiu et al (2022)* from Beijing Academy of Agriculture and Forestry Sciences fused GNSS and INS positioning information using an adaptive coefficient Kalman filtering algorithm, which improved the positioning accuracy by 47.7%. *Han et al (2017)* from Seoul National University in South Korea constructed an integrated system using three low-cost GPS receivers and inertial sensors, achieving a maximum positioning error of 0.64 m and a heading error of 2.1°. *Reitbauer and Schmied (2021)* from the United States proposed two multi-sensor fusion navigation algorithms for tracked agricultural vehicles, both of which can obtain sub-decimeter-level positioning accuracy. *Li et al (2021)* from China Agricultural University proposed a fuzzy adaptive finite impulse response Kalman filtering algorithm that fuses position and attitude information, which can effectively suppress Gaussian white noise in GNSS received signals and improve positioning accuracy. In view of the urgent demand for multi-crop combine harvester to adapt to complex planting patterns and the requirement of precision agriculture for operation accuracy, this paper takes a self-developed multi-crop combine harvester as the carrier to carry out the design and research of a high-precision positioning system and construct a precision positioning scheme. The aim is to improve the operation accuracy and environmental adaptability of the harvester, and promote the precise and efficient development of field operations of agricultural machinery.

MATERIALS AND METHODS

OVERALL STRUCTURE AND PRINCIPLE OF THE POSITIONING SYSTEM

The system is mainly composed of the main controller, the satellite positioning module, the attitude sensor, the 4G module, the storage module, the liquid crystal display module, the vehicle-mounted battery, the cloud server, and other components, as shown in Fig. 1.

The core functions of the designed NRTK Autonomous Positioning system are to obtain high-precision position, speeds, and attitude information of the harvester in real time. Its working principle is shown in Fig. 1, and the specific process is as follows: The ZED-F9P high-precision positioning module receives raw observation data from multi-system satellite positioning by the satellite antenna, and transmits the data to the STM32 main controller in real time through a Universal Asynchronous Receiver/Transmitter (UART) communication interface. The main controller parses the raw data and extracts key positioning data in the "GGA" format, which is then uploaded to the cloud service platform by the 4G communication module. After verifying the data for accuracy, the platform issues real-time differential correction data. The main controller forwards the differential data to the ZED-F9P module, which completes RTK positioning calculation by combining the satellite raw observation data with the differential correction data. Upon successful calculation, the system enters the fixed solution mode and outputs high-precision positioning data externally.

Meanwhile, the attitude sensor synchronously collects real-time attitude information of the harvester and transmits it to the STM32 main controller through a preset interface. The main controller performs unified parsing, time synchronization, and data fusion processing on the high-precision positioning data and attitude data. The core parameters are extracted such as latitude/longitude, instantaneous speed, and attitude angle, and outputted to accurately characterizing the real-time motion state of the harvester. In addition, the system is equipped with an SD card as the storage medium, which realizes bidirectional data interaction with the STM32 main controller through a Serial Peripheral Interface (SPI) communication interface. This enables reading, writing, and storage of key harvester data to support subsequent data traceability and analysis. The liquid crystal display module serves as a human-machine interaction terminal, presenting positioning data and system working status in real time through visualization—facilitating on-site operators to intuitively grasp equipment information. The power circuit module adopts a 16V-to-5V DC step-down module design. By connecting to the harvester's vehicle-mounted battery and undergoing step-down and voltage stabilization processing, it outputs a stable 5V DC power supply, providing reliable power support for all functional modules of the system and ensuring stable system operation.

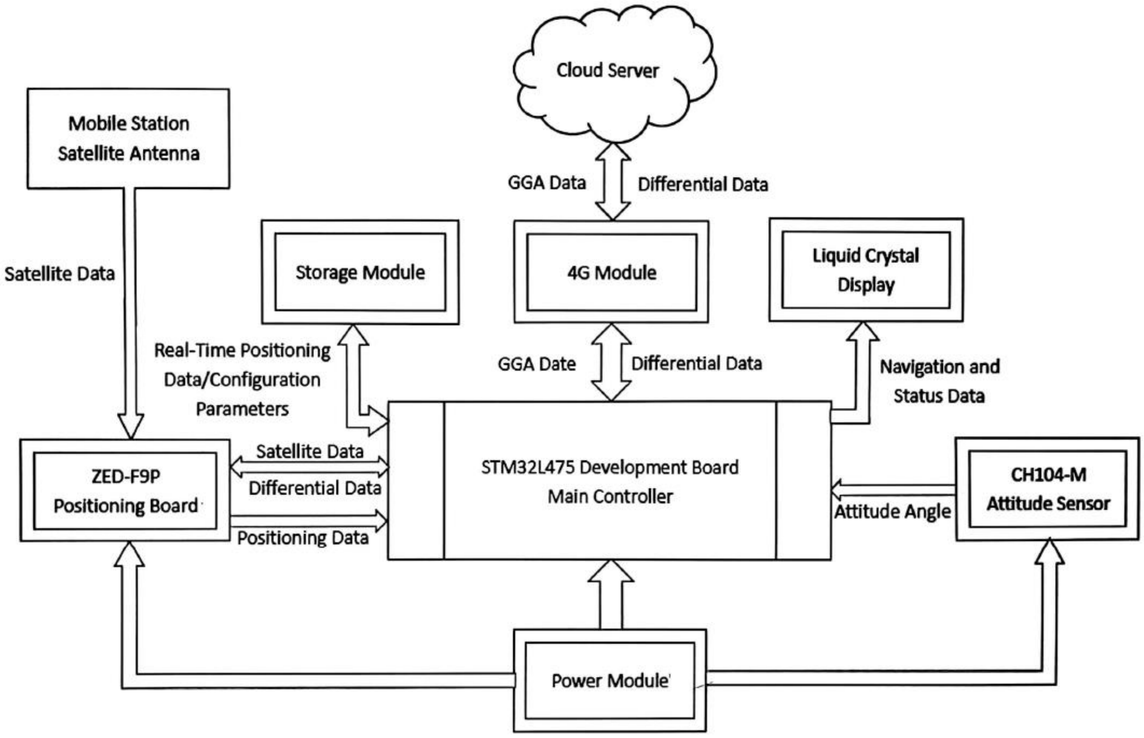

Fig. 1 - Working principle diagram of the NRTK autonomous positioning system

HARDWARE DESIGN AND SELECTION

In the NRTK autonomous positioning system, the controller serves as the core data processing unit, undertaking key tasks such as data parsing, data interaction scheduling among multiple modules, and data storage management. Its processing performance directly determines the overall response efficiency of the system and the reliability of data interaction. As shown in Fig. 2, a development board equipped with the STM32L475 microcontroller is selected as the system's core controller. This development board is equipped with a hardware Floating-Point Unit (FPU) and a Digital Signal Processing (DSP) instruction set, which can significantly improve the parsing efficiency and calculation accuracy of complex positioning data, and ensure the stability of real-time data interaction among multiple modules. Meanwhile, the development board integrates a 1.3-inch display screen and a TF card interface. The display screen enables real-time visual presentation of data, providing convenient human-machine interaction support for system program debugging and operation status monitoring; the TF card interface supports SD card access to realize local storage of positioning data.

As a core component of the autonomous positioning system, the satellite positioning module's core function is to receive multi-system satellite positioning signals and complete data parsing and processing. In high-precision positioning application scenarios, it also needs to have the capabilities of differential data reception and real-time calculation to achieve centimeter-level positioning accuracy output.

As shown in Fig.3, the designed RTK autonomous positioning system selects the ZED-F9P high-precision positioning module of the U-blox as the core component of satellite positioning. The specific performance parameters of this module are shown in Table 1.

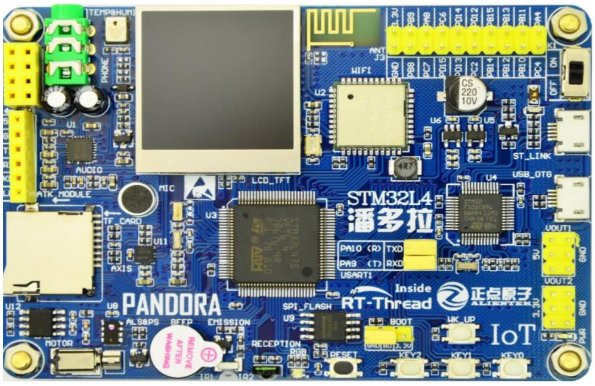

Fig. 2 - STM32L475 development

Fig. 3 - ZED-F9P High-precision positioning board

Table 1

Relevant parameters of ZED-F9P positioning module

Name	Parameters
Positioning Accuracy	Single - point Positioning Horizontal: 1.5 m Vertical: 2.5 m
	Differential Positioning Horizontal: 0.4 m Vertical: 0.8 m
	RTK Positioning Horizontal: 0.8 cm + 1 ppm; Vertical: 1.5 cm + 1 ppm
Speed Accuracy	0.05 m/s
Receivable Signal	BDS/GPS/GLONGASS/Galileo
Communication Protocol	UART, IIC
Data Format	Standard NMEA - 0183 Protocol Format
Update Frequency	20 Hz (Maximum)
Operating Voltage	5~12 V (DC)
Operating Current	300~1000 mA (DC)

In the NRTK autonomous positioning system, the bidirectional data interaction between local terminal data and the cloud service platform is a key link to ensure the realization of the system's high-precision positioning function, and directly affects the real-time performance and reliability of differential data transmission. Combining the system's demand for long-distance wireless communication, the study comprehensively considers core indicators such as communication link stability, data transmission rate, and environmental adaptability, and adopts an access scheme of "4G module + mobile cellular network" to achieve efficient data interaction between the local terminal and the cloud platform. As shown in Fig. 4, the EC800M-CN 4G module is selected as communication device, and the main performance parameters of this module are shown in Table 2.

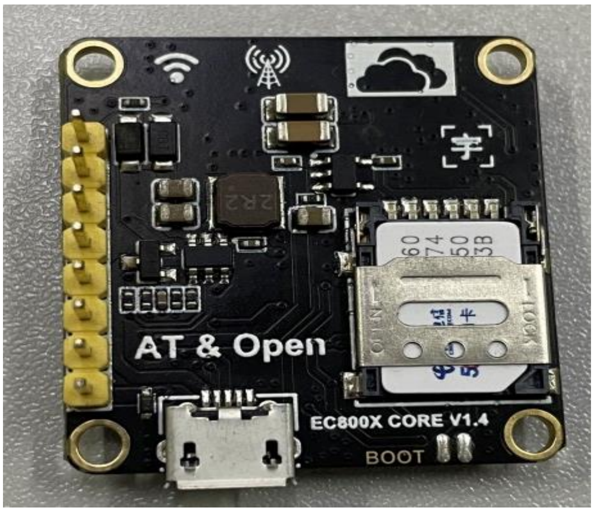

Fig. 4 - EC800M-CN 4G module

Fig. 5 - CH104 attitude sensor

Table 2
Relevant parameters of EC800M-CN 4G module

Name	Parameters
Network Standard	Supports 4G networks of China Mobile/China Unicom / China Telecom
Communication Rate	Maximum downlink rate: 10 Mbps, Maximum uplink rate: 5 Mbps
Power Supply	Voltage: 5 – 12 V (DC), Current: Not less than 1000 mA (DC)
Communication Interface	UART (compatible with 3.3 V and 5 V), Baud rate: 4800 – 921600 bps
Supported Protocol	TCP/UDP/MQTT/HTTPS
Operating Temperature	-35 ℃ ~ +75 ℃

In the RTK positioning technology system, the core difference between the traditional RTK system and the NRTK system lies in the transmission link and supply mode of differential data. For the designed NRTK positioning system, the differential data is provided by the cloud service platform. The system establishes a stable connection with Qianxun Location Network through the 4G network and uploads the terminal position information at a preset frequency. After receiving the data, Location Network calculates the rough position of the positioning terminal, and then issues the corresponding differential correction data to the system terminal in a targeted manner, providing data support for high-precision positioning. Since the satellite positioning module selected in this system only connects to a single satellite antenna, it can only obtain single-point position information and cannot calculate heading data. Therefore, an additional attitude sensor is required to collect the attitude angle parameters of the harvester. As shown in Fig. 5, considering the engine vibration noise interference and body jolting at the complex field road conditions during the harvester operation, the industrial-grade CH104 series attitude sensor is selected as the attitude data collection unit. Its specific performance parameters and technical indicators are shown in Table 3.

Table 3
Relevant parameters of CH104 attitude sensor

Parameters	**Parameter values**
Data Update Frequency	400 Hz (Maximum)
Attitude Angle Full - Scale Range	Heading Angle: -180° ~ +180° Pitch Angle, Roll Angle: -90° ~ +90°
Attitude Angle Output Accuracy	Pitch Angle, Roll Angle, Heading Angle: ±0.2°
Communication Protocol	CAN, RS232/485
Operating Temperature	-40 ℃ ~ +85 ℃
Operating Voltage	5 ~ 36 V (DC)
Power Consumption	Less than 500 mW

SOFTWARE DESIGN PROCESS

The software of the designed NRTK autonomous positioning system adopts a "functionality-oriented" embedded development concept, with the core goal of meeting the actual operational needs of high-precision autonomous positioning for harvester. The C language is used as the programming language, and it is paired with the KEIL compiler to complete code compilation, debugging, and ensuring the efficiency and portability of the program. The core functional modules of the software system are divided into five major modules, specifically including: the system initialization module, the positioning data processing module, the attitude sensor data processing module, the human-machine interaction display module, and the data storage module. The basic software workflow of the autonomous positioning system is shown in Fig. 6.

Its core execution logic is as follows: After the system powered on, it first enters the initialization phase to complete the initial configuration of hardware resources such as the microcontroller, peripheral interfaces, communication modules, and storage units. Upon completion of initialization, the DMA (Direct Memory Access) UART interrupt reception function is activated, and the system then enters the main loop mode. During the main loop cycle, the system asynchronously receives positioning data and attitude sensor data by the UART, with the positioning data update frequency set to 5 Hz and the attitude sensor data update frequency set to 10 Hz. When the system detects that the reception of positioning data or attitude sensor data is completed, it immediately triggers the corresponding data processing flow. In the positioning data processing flow, the data segments required for business operations are first accurately filtered from the received raw positioning data, and then the core parameters required for high-precision autonomous positioning are extracted in a targeted manner. The output data of the ZED-F9P satellite positioning module adopts the standard NMEA-0183 protocol format and uses Beidou/GPS dual-mode combined satellite data, with the corresponding universal sentence prefix uniformly set to "GN".

After filtering and extraction of key parameters, the positioning data is further optimized through algorithms such as filtering, calibration, format conversion, and data fusion. Upon completion of data processing, the system synchronously executes multi-dimensional data output operations, including real-time visual display of data by the display module, data transmission to external devices by the communication interface, and local archiving of key data by the storage module, to ensure the real-time performance, traceability, and availability of the data. The harvester only requires position and speed information during operation, so the satellite positioning module can output only GGA and VTG data to reduce data volume. Among them, GGA data is used for local position parsing and uploading to the cloud server by the 4G module to obtain differential signals; The VTG data is used for acquiring real-time speed. As shown in Fig. 7, the core of positioning data processing lies in the parsing of GNGGA and GNVTG data, including data validity judgment and key data extraction. The CH104 attitude sensor communicates with the main controller by the UART, to transmit data according to a specific frame structure, and to complete data parsing. Human-machine interaction is realized by driving the LCD screen to display data through SPI communication, and data storage is realized by the main controller reading and writing to the SD card based on the FATFS file system.

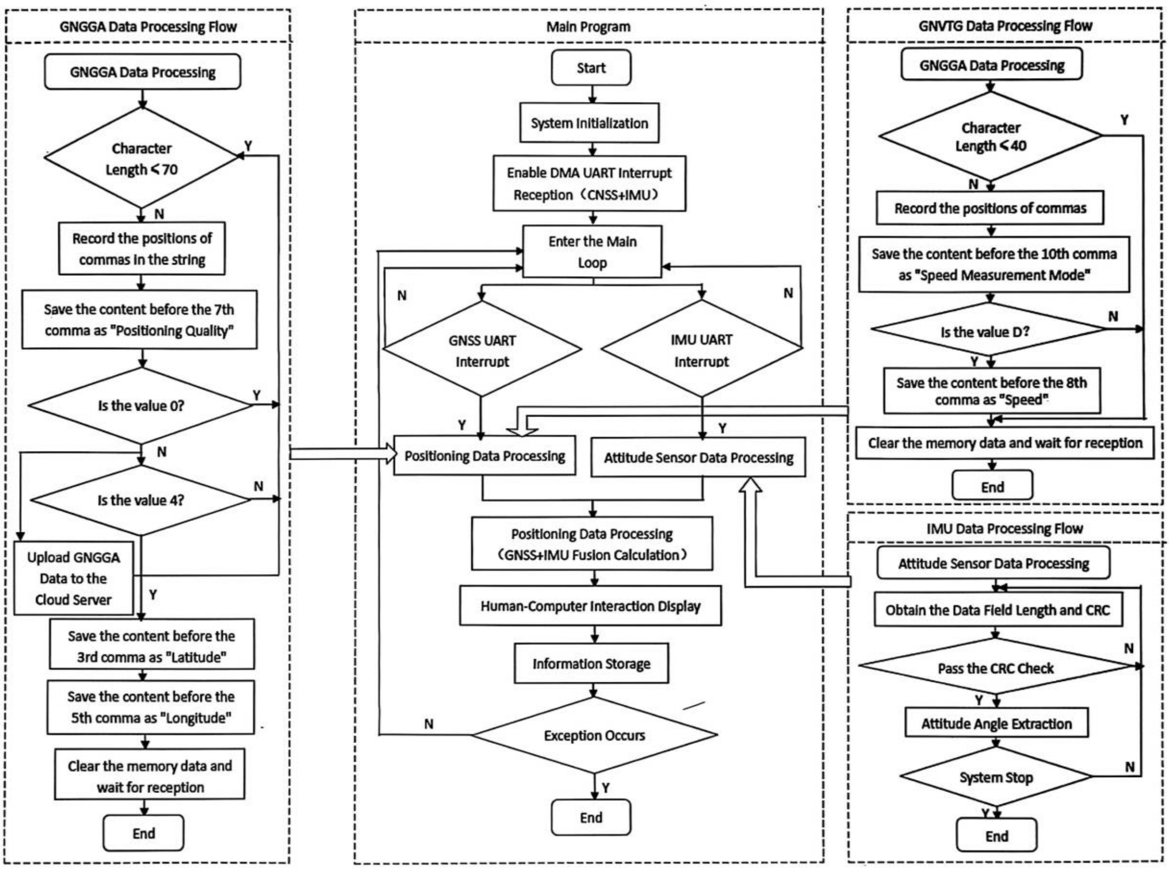

Fig. 6 - Workflow diagram of NRTK autonomous positioning system

ESTABLISHMENT AND CORRECTION OF THE VEHICLE BODY COORDINATE SYSTEM

The harvester obtains latitude and longitude information in the WGS-84 coordinate system through the positioning module. To meet the requirements of path planning, position measurement, and error analysis in actual operations, the Gauss-Kruger projection method is used to convert the latitude and longitude into plane rectangular coordinates. Since the harvester's heading angle obtained by the attitude sensor is only related to its own motion state, the reference path planning is based on the vehicle body coordinate system, which takes the geometric center of the harvester as the origin. The forward direction of the attitude sensor when powered on is the positive direction of the horizontal axis Xc, and the direction on the left side of the harvester that is perpendicular to the forward direction and passes through the geometric center is the positive direction of the vertical axis Yc. The conversion relationship between the Gauss plane coordinate system and this vehicle body coordinate system is shown in Fig. 7.

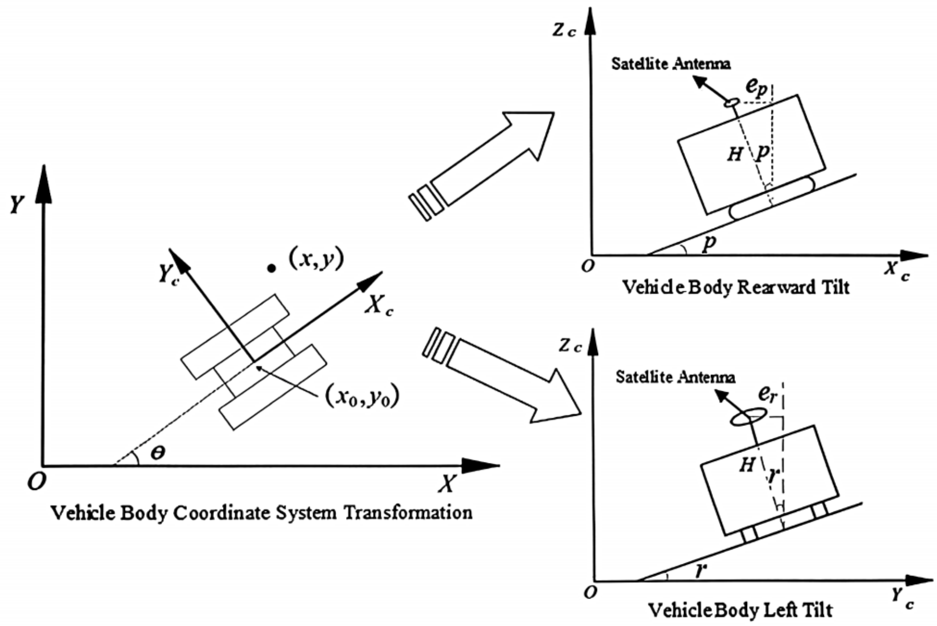

Fig. 7 - Schematic diagram of diagram of vehicle body coordinate transformation and correction

As can be seen from Fig. 7, the coordinate values of a point (x, y) in the Gauss plane under the vehicle body coordinate system can be calculated using the following formula:

$$\begin{bmatrix} x_c \\ y_c \end{bmatrix} = \begin{bmatrix} x - x_0 & y - y_0 \\ y - y_0 & -x + x_0 \end{bmatrix} \begin{bmatrix} \cos\theta \\ \sin\theta \end{bmatrix} \tag{1}$$

In the formula (1):

x_c, y_c —The coordinate values of the point (x, y) in the Gauss plane under the vehicle body coordinate system, m;

x_0, y_0 —The coordinate values of the harvester's geometric center in the Gauss plane coordinate system, m;

θ —The angle between the horizontal axis of the vehicle body coordinate system and the horizontal axis of the Gauss plane coordinate system, °.

During operation, tilting of the harvester body causes the satellite antenna to undergo horizontal displacement relative to its initial position, which leads to deviations in the positioning system measurement data. When the tilt angle becomes large, these deviations can result in significant positioning errors, thereby degrading path tracking performance. Therefore, it is necessary to correct the positioning errors induced by vehicle body tilt. As shown in Fig. 7, when the harvester travels along the positive direction of the horizontal axis of the vehicle body coordinate system and tilts backward, the satellite antenna shifts toward the negative direction of the horizontal axis, resulting in the measured position lagging the actual position along the horizontal axis. When the harvester travels along the positive direction of the vertical axis and tilts backward, the satellite antenna shifts toward the negative direction of the vertical axis, causing the measured position to lag the actual position along the vertical axis. When the harvester tilts forward, the measured position is ahead of the actual position along both the horizontal and vertical axes. As shown in Fig. 7, when the harvester travels along the positive direction of the horizontal axis of the vehicle body coordinate system and tilts to the left, the satellite antenna shifts toward the negative direction of the vertical axis, leading to a lag of the measured position relative to the actual position along the vertical axis. When the harvester travels along the positive direction of the vertical axis of the vehicle body coordinate system and tilts to the left, the satellite antenna shifts toward the positive direction of the horizontal axis, resulting in the measured position being ahead of the actual position along the horizontal axis. When the harvester tilts to the right along the horizontal or vertical axis, its measured position will be ahead along the vertical axis or lag along the horizontal axis. After correcting the attitude error, the coordinate value of any position of the harvester in the Gauss plane corresponding to the vehicle body coordinate system is:

$$\begin{bmatrix} x_c \\ y_c \end{bmatrix} = \begin{bmatrix} x - x_0 & y - y_0 \\ y - y_0 & -(x - x_0) \end{bmatrix} \begin{bmatrix} \cos\theta \\ \sin\theta \end{bmatrix} + \begin{bmatrix} e_p & -e_r \\ e_r & e_p \end{bmatrix} \begin{bmatrix} \cos\varphi \\ \sin\varphi \end{bmatrix} \tag{2}$$

In the formula (1): e_p—Pitch Angle Error, m; e_r—Roll Angle Error, m; p—Harvester Pitch Angle, °; r—Harvester Roll Angle, °; φ—Harvester Heading Angle, °.

PERFORMANCE TESTING SCHEME

Position Accuracy Test

Test Purpose: To determine the positioning accuracy of the autonomous positioning system and verify whether it meets the high-precision positioning requirements during the harvester's path tracking process.

Test Method: Drive the harvester to an open outdoor area and ensure that all components of the autonomous positioning system are correctly installed and the software is properly configured. Set the output frequency of the positioning system to 5 Hz. After the system enters the fixed solution mode, collect real-time positioning data for more than 30 minutes. Subsequently, perform post-processing and analysis on the collected positioning data.

The Circular Error Probable (CEP) and Double Distance Root Mean Square ($2DRMS$) are used as the accuracy evaluation indicators for the positioning system, and the calculation formulas are as follows:

$$\begin{cases} CEP = 0.62\sigma_y + 0.56\sigma_x \\ 2DRMS = 2\sqrt{\sigma_x^2 + \sigma_y^2} \end{cases} \tag{3}$$

In the formula (3):

CEP—Circular Error Probable, m, fifty percent of the positioning points will fall within the circle with the CEP as its radius.

$2DRMS$—Double Distance Root Mean Square, m, between 95.8% and 98.2% of the positioning points will fall within the circle with 2DRMS as its radius.

σ_x, σ_y—The standard deviation of the X-coordinate and the standard deviation of the Y-coordinate for the measured data samples.

Speed Measurement Test

Test Purpose: To verify the speed measurement accuracy of the system by comparing the manual measured with the system measured speed of the harvester.

Test Method: The field test of the high-precision positioning system for combine harvester strictly followed the requirements in *Harvesting machinery — Combine harvesters — Test procedures and performance evaluation (State Administration for Market Regulation (SAMR), 2025)*. During the test, the harvester shall be in a no-load state with the power transmission of the threshing body and the header assembly disconnected, and the test site shall be a flat hard road surface. A straight road section with a length of 50 meters shall be testing on the flat road surface as the speed measurement section. Along the speed measurement section, a measuring point shall be set every 10 meters from the starting point to the end point. In addition, a preparation section and a buffer section of about 5 meters each shall be set before and after the speed measurement section. The preparation section is used for turning on the positioning system, starting the harvester, accelerating, etc., while the buffer section is used for decelerating and buffering after the speed measurement is completed. Three gears were designed for the test: low-speed driving (approximately 0.4 m/s), medium-speed driving (approximately 0.8 m/s), and high-speed driving (approximately 1.2 m/s). Each speed was tested four times, and 5 speed measuring points were fixedly arranged for each test. During the test, the harvester first starts and accelerates on the preparation section. When the speed is stable, the harvester drives into the speed measurement section at a constant speed. From the moment it enters the speed measurement section, the time required for the harvester to reach each measuring point is recorded. A speed measurement test is completed only after the entire harvester body has completely driven out of the speed measurement section.

RESULTS AND ANALYSIS

The duration of the positioning accuracy test was approximately 40 minutes, and a total of 11,995 valid positioning data points were obtained. The post-processing of the positioning data yielded the following results: $\sigma_x = 0.00626$, $\sigma_y = 0.00459$.

Substituting these values into Formula (3) yields:

$$\begin{cases} CEP = 0.62 \times 0.00459 + 0.56 \times 0.00626 = 0.00638\ m \\ 2DRMS = 2 \times \sqrt{0.00459^2 + 0.00626^2} = 0.0156\ m \end{cases} \tag{4}$$

The test and analysis results are shown in Fig. 8. As shown in Fig. 8(b), the small dots represent all positioning scatter points, and there are a large number of overlapping data points. The radius of big circle is approximately 1.56 cm, indicating that 95.8% to 98.2% of the positioning scatter points fall within the circle. The calculation results based on the formula (4) show that the positioning error of the designed NRTK autonomous positioning system is less than 2 cm, and its positioning accuracy meets the high-precision positioning requirements during the harvester's path tracking process.

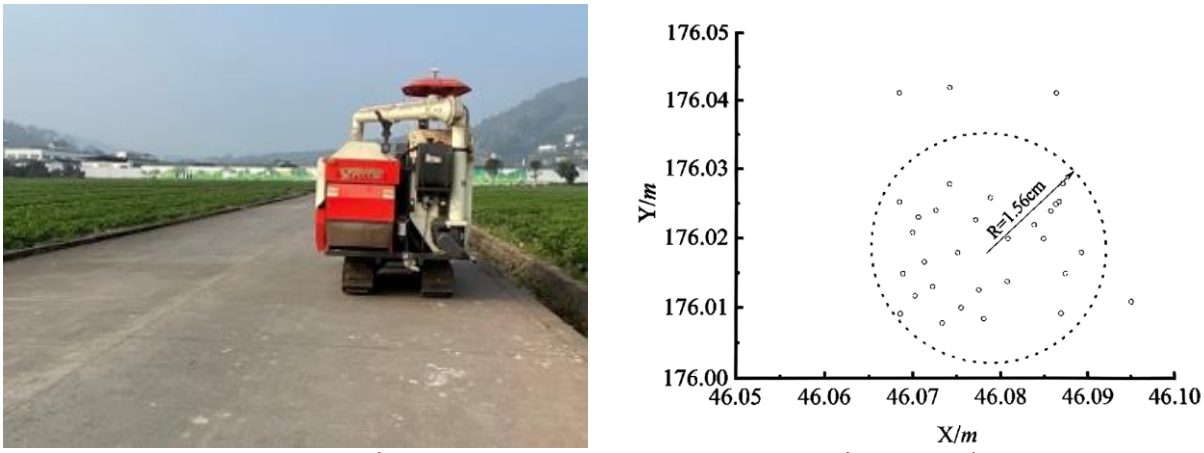

(a) Testing Equipment and Scenarios *(b) Scatter Plot of Test Results*

Fig. 8 - Autonomous positioning system positioning accuracy test

The speed measurement test results of the positioning system are shown in Fig. 9, and the analysis results are shown in Fig. 10.

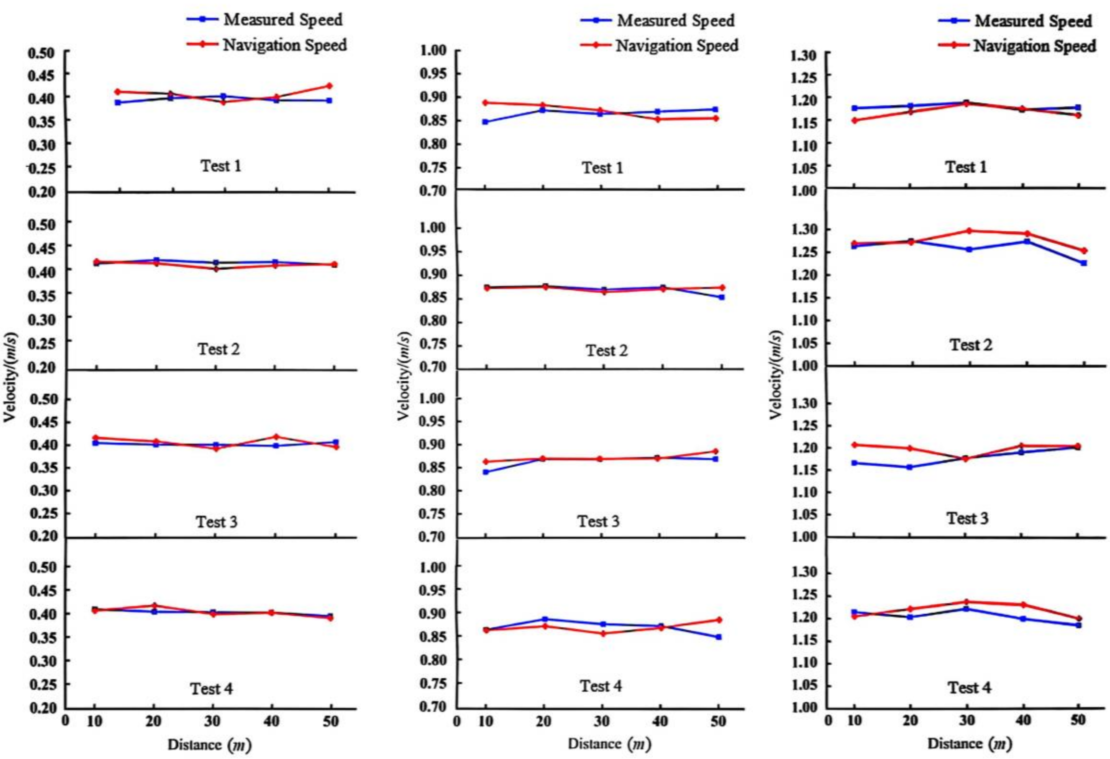

(a) Low-speed group *(b) Medium-speed group* *(c) High-speed group*

Fig. 9 - Test results of Harvester at different travel speeds

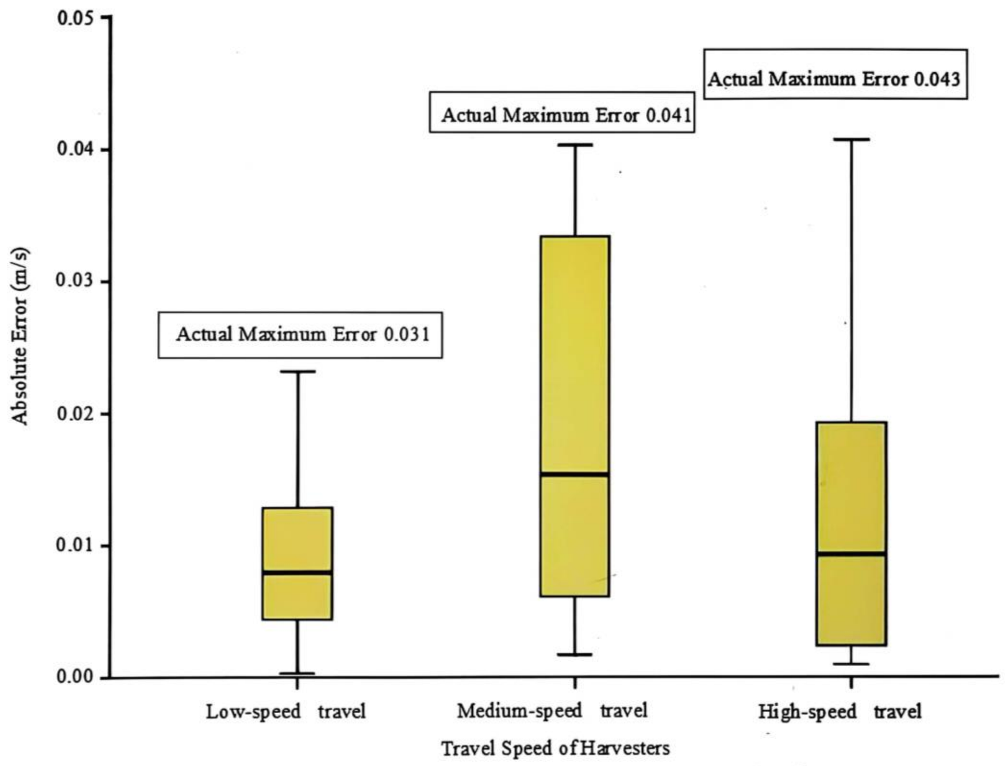

Fig. 10 - Comparison of measurement accuracy of Harvester at different travel speeds

The test results show that the speed measurement error of the autonomous positioning system changes significantly with the speed increases. When low-speed driving, the maximum measurement error is 0.031 m/s, and the average error is 0.010 m/s. When medium-speed driving, the maximum errors are 0.041 m/s and the average error 0.013 m/s. When high-speed driving, the maximum errors are 0.043 m/s and the average error 0.019 m/s. Under low-speed conditions, the measurement accuracy is significantly better than that under medium and high speeds. Data concentration, test reproducibility, and stability are all optimal at low-speeds. The errors are generally biased toward small values, with the lowest median error, the narrowest reasonable error upper limit and fluctuation range, the lowest risk of extreme errors, and the best error controllability. Under medium-speed driving, the discrete range of core errors is the largest, with obvious error fluctuations and the highest median error. The reasonable error upper limit and the risk of extreme errors are at a moderate level, and the stability is the worst. Under high-speed driving, the core error dispersion is the largest, and the reasonable error upper limit, fluctuation range, and actual maximum error are all the largest; the risk of extreme errors is significant, and the stability is moderate. Comprehensive analysis indicates that accuracy and reliability show a significant deterioration trend with the increase of the speed. Low-speed driving achieves high stability, a tendency toward small errors, a low reasonable error upper limit, and a low risk of extreme errors. It also exhibits excellent positioning repeatability and error controllability, and meets the requirements for high-precision positioning system. Medium-speed driving provides overall accuracy and stability that can meet the needs of conventional positioning scenarios. High-speed driving results that the stability is relatively poor, the risk of extreme deviations is significant, and the overall reliability is moderate. The reasons can be summarized as follows. Under low-speed conditions, the satellite signal reception is stable, the dynamic error accumulation of IMU is slow, the sensor data noise is low, and the vehicle attitude changes gently, and the positioning algorithm has enough time to complete data fusion and deviation correction. Under medium-speed conditions, the synchronization between sensor data update rates and vehicle attitude variations decreases. Minor signal delays occur under certain operating conditions, resulting in reduced efficiency of algorithmic deviation correction. Under high-speed conditions, satellite signal reception quality degrades significantly, IMU accumulated errors increase rapidly, and sensor data accuracy deteriorates. Real-time dynamic adjustment of the positioning algorithm becomes more challenging, revealing limitations in the system’s dynamic adaptability to high-speed scenarios and in the optimization of algorithm parameters. In addition, intrinsic speed measurement errors of the positioning system and reaction time errors associated with manual measurements also contribute to the observed deviations.

CONCLUSIONS

This study focuses on the research and development of a harvester positioning system, and completes a series of key research work, achieving significant results.

(1) The overall design framework of the harvester positioning system is constructed. This study systematically sorts out and in-depth analyzes the functional positioning and core working principles of each component module in the system, laying a solid theoretical and structural foundation for the subsequent development and implementation of the system.

(2) The design of the positioning system based on NRTK technology is completed. The study conducts in-depth analysis on the key workflow of the system, namely "satellite signal reception - differential data transmission - positioning result calculation", clarifying the technical logic and implementation path of high-precision positioning. Meanwhile, the selection and matching of core hardware for the positioning system are completed, and the development of software functional modules are realized. On this basis, the optimized design of coordinate transformation and the correction of harvester attitude errors are carried out, which effectively improves the accuracy and environmental adaptability of positioning data, ensuring the stability and reliability of the system in practical operation.

(3) Performance test results shows that the positioning error of the developed system is less than 2 cm, which fully meets the requirements of high-precision positioning for harvesters. When the harvester operates at a typical speed range of 0.4-1.2 m/s, the maximum speed measurement error of the system is less than 0.05 m/s, and the average speed measurement error is about 0.014 m/s. All performance indicators have reached the precision requirements of the harvester positioning system.

ACKNOWLEDGEMENT

The study was Supported by the Natural Science Research Projects of Universities in Anhui Province (2023AH040222), the Chengdu Science and Technology Project (2024-YF09-00035-SN), and the Sichuan Innovation Team of Chinese National Modern Agricultural Industry Technology System (SCCXTD-2026-21(27)).

REFERENCES

[1] Chen, X.D., Liu, H., Wei, B.G., Sheng, C.Q., Huang, G.W., Hui, S.Y., & Ying, J.J. (2025). Bei Dou/GNSS Wide-Area precise positioning technology and service: current situation and prospects (北斗/GNSS 广域精密定位技术与服务:现状与展望). *Geomatics and Information Science of Wuhan University*, *50*(3), 413-429. https://doi.org/10.13203/j.whugis20230472

[2] Cheng, Z., Gong, T., Liang, M., Wang, Y. (2025) Key Technologies of Intelligent Legume Harvesting Equipment Based on BeiDou Navigation and 5G+MEC. *Packaging Engineering,* 46(16): 552-559 https://doi.org/10.19554/j.cnki.1001-3563.2025.16.050

[3] Choi, J., Lee, B., & Jung, H. (2024). Development of a retrofit autonomous maneuvering system for agricultural vehicles. *2024 IEEE International Automated Vehicle Validation Conference (IAVVC),* 1-4. https://doi.org/10.1109/iavvc63304.2024.10786403

[4] Hammou, N. A., Mousannif, H., Lakssir, B., Harkani, A., & Elaissaoui, A. (2025). Implementation of a low-cost vision method for autonomous navigation of agricultural robots. *International Review of Automatic Control, 18(3),* https://doi.org/10.15866/ireaco.v18i3.26062

[5] Han, X., Kim, H.J., Jeon, C.W., Moon, H.C., & Kim, J.H. (2017). Development of a low-cost GPS/INS integrated system for tractor automatic navigation. *International Journal of Agricultural and Biological Engineering*, *10*(2), 123-131. https://doi.org/10.3965/j.ijabe.20171002.3070

[6] He, J., He, J., Luo, X.W., Li, W.C., Man, Z.X., & Feng, D.W. (2022). Rice Row Recognition and Navigation Control Based on Multi-sensor Fusion (基于多传感器融合的水稻行识别与跟踪导航研究). *Transactions of the Chinese Society for Agricultural Machinery*, *53*(3), 18-26, 137. https://doi.org/10.6041/j.issn.1000-1298.2022.03.002

[7] Li, S., Zhang, M., Ji, Y., Zhang, Z., Cao, R., Chen, B., Li, H., & Yin, Y. (2021). Agricultural machinery GNSS/IMU-integrated navigation based on fuzzy adaptive finite impulse response Kalman filtering algorithm. *Computers and Electronics in Agriculture*, *191*, 106524. https://doi.org/10.1016/j.compag.2021.106524

[8] Meng, Z.J., Wang, H., Fu, W.Q., Liu, M.N., Yin, Y.X., & Zhao, C.J. (2023). Research Status and Prospects of Agricultural Machinery Autonomous Driving (农业装备自动驾驶技术研究现状与展望).

Transactions of the Chinese Society for Agricultural Machinery, *54*(10), 1-24. http://doi.org/10.6041/j.issn.1000-1298.2023.10.001
[9] Qiu, Q., Hu, Q.H., Fan, Z.Q., Sun, N., & Zhang, X.H. (2022). Adaptive-Coefficient Kalman Filter-Based Combined Positioning Algorithm for Agricultural Mobile Robots (基于自适应系数卡尔曼滤波的农业移动机器人组合定位). *Transactions of the Chinese Society for Agricultural Machinery*, *53*(S1), 36-43. http://doi.org/10.6041/j.issn.1000-1298.2022.S1.004
[10] Raikwar, S., Fehrmann, J., & Herlitzius, T. (2022). Navigation and control development for a four-wheel-steered mobile orchard robot using model-based design. *Comput. Electron. Agric., 202,*107410. https://doi.org/10.1016/j.compag.2022.107410
[11] Reitbauer, E., & Schmied, C. (2021). Performance Analysis of GNSS/INS/VO/Odometry Sensor Fusion Algorithms for Tracked Agricultural Vehicles. *Proceedings of the 34th International Technical Meeting of the Satellite Division of The Institute of Navigation (ION GNSS+ 2021)*, St. Louis, Missouri, 3250-3262. https://doi.org/10.33012/2021.18053
[12] Saha, S. , Morita, T. , & Noguchi, O. N. (2022). A vision-based navigation system for an agricultural autonomous tractor. *ifac papersonline, 55(32)*, 48-53. https://doi.org/10.1016/j.ifacol.2022.11.113
[13] Schütte,T., Koch, K., Dworak, V., Weltzien, C. (2023). Lidar assisted semi-automatic mapping and path planning approach for autonomous mobile robots in vineyards and orchards. *LAND.TECHNIK AgEng 2023*, 199-208. https://doi.org/10.51202/9783181024270-199
[14] State Administration for Market Regulation (SAMR), Standardization Administration of the People's Republic of China (SAC). *Harvesting machinery—Combine harvesters—Test procedures and performance evaluation*, GB/T 8097-2025. Beijing: Standards Press of China, 2025.
[15] Udompant, K., Ospina, R., Kim, Y.J., & Noguchi, N. (2021). Utilization of quasi-zenith satellite system for navigation of a robot combine harvester. *Agronomy*, *11*(3), 483. https://doi.org/10.3390/agronomy11030483
[16] Xiao, R.H., Ma, X., Li, H.W., Cao, X.L., Wei, Y.H., Wang, C.E., & Zhao, X. (2022). Design and experiment of agricultural machinery auxiliary navigation system based on UWB positioning (基于 UWB 定位的农业机械辅助导航系统设计与试验). *Journal of South China Agricultural University*, *43*(3), 116-123. http://doi.org/10.7671/j.issn.1001-411X.202107049
[17] Yang, S.Y., Song, Y., Xue, J.L., & Wang, P.X. (2024). Multi-sensor integrated positioning of rice transplanter based on visual supplementation (基于视觉补充的水稻插秧机多传感器组合定位研究). *Journal of Huazhong Agricultural University*, *43*(2), 234-246. http://doi.org/10.13300/j.cnki.hnlkxb.2024.02.026
[18] Zhang, Z.G., Yin, Z., Wu, X., Liu, J., Hu, L., Zhang, W.Y., He, J., Tong, Z.Y., Liu, C.K., & Luo, X.W. (2025). Research progress on the automatic navigation technology for agricultural machinery (农业机械自动导航技术研究进展). *Transactions of the Chinese Society of Agricultural Engineering*, *41*(23), 1-13. http://doi.org/10.11975/j.issn.1002-6819.202505262
[19] Zhao, P., Li, F.T., Zang, L., Liang, B., Cai, B., (2024). Beidou High-Precision Navigation and Positioning Technologies and Applications under 5G Conditions (5G 条件下北斗高精度导航定位技术与应用). *Journal of Geomatics*, 2024, 49(1): 88-90. https://doi.org/10.14188/j.2095-6045.20230461
[20] Zhong, Y., Xue, M.Q., & Yuan, H.L., (2021). Design of the GNSS/INS integrated navigation system for intelligent agricultural machinery (智能农机 GNSSINS 组合导航系统设计). *Transactions of the Chinese Society of Agricultural Engineering*, *37*(9), 40-46. https://doi.org/10.11975/j.issn.1002-6819.2021.09.005